[AMERICAN JOURNAL OF SCIENCE, VOL. 267, OCTOBER, 1969, P. 945-968]

PARTITIONING OF Fe^{++} AND Mg^{++} BETWEEN COEXISTING SYNTHETIC OLIVINE AND ORTHOPYROXENE

L. G. MEDARIS, JR.

Department of Geology and Geophysics, University of Wisconsin, Madison, Wisconsin 53706

ABSTRACT. Using standard hydrothermal equipment, partitioning of Fe^{++} and Mg^{++} between olivine and orthopyroxene has been investigated at 900° and 800°C, at a total fluid pressure of 500 bars and oxygen fugacities defined by the fayalite–magnetite–quartz buffer. Coexisting olivine and orthopyroxene were synthesized from oxide starting mixes, and equilibrium was closely approached by making reversal runs in which Fe^{++} and Mg^{++} were exchanged between previously crystallized pure olivine and orthopyroxene of initially different Fe:Mg ratios in the presence of H_2O or 2M (Fe,Mg) Cl_2 solutions. Compositions of run products were determined by measurement of d_{130} in olivine and d_{610} in orthopyroxene. Partitioning at 900°C is expressed by the best-fit equation

$$\log\left(\frac{X_{Fe}}{X_{Mg}}\right)_{OL} = 0.1630 + 1.1128 \log\left(\frac{X_{Fe}}{X_{Mg}}\right)_{OPX}$$

Coexisting olivine and orthopyroxene were also synthesized from starting mixes containing ferrous oxalate at 900°, 800°, and 700°C, at a total fluid pressure of 500 bars, but oxygen fugacity was not controlled, nor have the runs been reversed. These data are, however, compatible with those in which a close approach to equilibrium was attained.

Comparison of experimental data with published experimental data at liquidus temperatures demonstrates that Fe^{++}–Mg^{++} partitioning between olivine and orthopyroxene is not appreciably temperature dependent over the interval 900° to 1300°C and possibly over the range 700° to 1300°C.

There is close agreement between partitioning determined by experiment and that predicted on the basis of cation exchange between an ideal single-site phase (olivine) and a double-site phase (orthopyroxene) in which there is ideal solution behavior between the sites. At 900°C the change in standard free energy, $\Delta G_T°$, for exchange of Fe^{++} and Mg^{++} between olivine, and orthopyroxene is −1750 cal/gfw and the change in standard free energy, $\Delta G_E°$, for exchange of Fe^{++} and Mg^{++} between M_1 and M_2 in orthopyroxene is −2940 cal/gfw.

Although the compositions of coexisting olivine and orthopyroxene cannot be used to estimate temperatures of equilibration in igneous or metamorphic rocks, comparison of the compositions of these minerals with the experimental partitioning curve is useful in interpreting whether or not these silicates are in equilibrium. This approach is illustrated with data on olivine–orthopyroxene pairs from chondritic meteorites, stratiform basic intrusives, peridotite nodules from basalt and kimberlite, and alpine peridotites.

INTRODUCTION

In recent years there has been a great deal of interest in partitioning of elements between coexisting phases as a means of interpreting the conditions of formation of igneous and metamorphic rocks. The pioneering paper on element partitioning in minerals was published in 1951 by Ramberg and DeVore, who studied the distribution of Fe^{++} and Mg^{++} between olivine and orthopyroxene. This mineral pair is particularly suitable for investigation because the chemistry is relatively simple, and the two minerals are associated in a variety of rock types, including chondritic meteorites, alpine peridotites, gabbros and peridotites from stratiform complexes, peridotite nodules in basalt and kimberlite, and certain metamorphic rocks. From thermodynamic arguments Ramberg

and DeVore concluded that Fe^{++}–Mg^{++} partitioning between equilibrium pairs of olivine and orthopyroxene is relatively insensitive to changes in pressure, but that partitioning should be sensitive to variations in temperature, and thus might serve as a useful geothermometer.

Since the appearance of Ramberg and DeVore's paper, naturally occurring olivine–orthopyroxene assemblages have been investigated by Ross, Foster, and Myers (1954), Ringwood (1961), Bartholomé (1962), O'Hara (1963), Keil and Fredriksson (1964), and Van Schmus and Koffman (1967), among others. Craig (1964) and Mueller (1964) attempted to predict the effect of temperature on Fe^{++}–Mg^{++} partitioning on the basis of thermodynamic considerations, utilizing data from experimental studies by Bowen and Schairer (1935), Muan and Osborn (1956), and Ernst (1960). However, because none of these experimental studies was specifically designed to investigate element partitioning, there were insufficient data available for the precise determination of the temperature dependence of partitioning.

The purpose of this study was to investigate partitioning of Fe^{++} and Mg^{++} between synthetic olivine and orthopyroxene hydrothermally at subsolidus temperatures and to evaluate partitioning as a function of temperature.

Since this investigation was completed, Speidel and Osborn (1967), Nafziger and Muan (1967), and Larimer (1968) have reported results on element partitioning between olivine and orthopyroxene at liquidus temperatures. Thus, partitioning data over a range of almost 600°C are now available, and the possible use of Fe^{++}–Mg^{++} partitioning between olivine and orthopyroxene in geothermometry may now be evaluated.

ACKNOWLEDGMENTS

This investigation was carried out in 1965 and 1966 while I was a National Science Foundation Postdoctoral Fellow at the Department of Geology, University of California, Los Angeles. I am indebted to W. G. Ernst for his direction and encouragement throughout this study and for his making available laboratory facilities supported by National Science Foundation Research Grant GP-5058. J. E. Grover, J. W. Larimer, and W. R. Van Schmus furnished preprints that were invaluable in preparation of this paper. All the people mentioned above kindly reviewed the manuscript and contributed to its improvement.

EXPERIMENTAL PROCEDURE

Standard hydrothermal techniques were used in this investigation. All runs were made in cold seal pressure vessels at a total fluid pressure of 500 bars. Each charge was sealed with excess H_2O inside a $Ag_{70}Pd_{30}$ capsule, and oxygen fugacity was controlled by placing the $Ag_{70}Pd_{30}$ capsule, fayalite–magnetite–quartz buffer, and excess H_2O within a Au capsule. The oxygen fugacity defined by this buffer system is $10^{-12.92}$ bars at 900°C, 500 bars fluid pressure, and $10^{-14.95}$ bars at 800°C, 500 bars (Wones and Gilbert, 1967; Eugster and Wones, 1962). Because the dura-

tion of runs ranged up to 800 hrs, each run was interrupted at intervals of about 150 hrs to check and replace the buffer, for optical and X-ray examination of the charge, and for grinding the charge in an agate mortar to facilitate complete reaction.

Coexisting olivine and orthopyroxene were synthesized at 900° and 800°C from oxide starting mixes composed of cristobalite, periclase, and metallic iron. However, there was no assurance that the compositions of the two minerals in these synthesis assemblages represented equilibrium compositions. Accordingly, previously synthesized pure olivine and orthopyroxene with appreciably different Fe:Mg ratios were mixed and equilibrated in sealed, buffered $Ag_{70}Pd_{30}$ capsules, in which either H_2O or 2M $(Mg,Fe)Cl_2$ solutions served as the medium for cation exchange between the two phases. By this method the equilibrium distribution of Fe^{++} and Mg^{++} between the two phases was closely approached at both 900° and 800°C. The idea for using chloride solutions as an exchange medium was stimulated by Orville's (1963) successful use of 2M (Na,K)Cl solutions in an experimental study of alkali feldspars. Solutions of $MgCl_2$ and $FeCl_2$ are suitable for experiments with olivine and orthopyroxene because both chlorides are extremely soluble in H_2O, and the ionic radius of chlorine (1.81Å) is too large for chlorine to be incorporated in the silicate structures.

An attempt was made to synthesize coexisting olivine and orthopyroxene from oxide starting mixes at 700°C, but orthopyroxene was unstable at this temperature in the presence of H_2O, and hydrous phases appeared in the run products. Synthesis assemblages consisted of olivine–talc, olivine–talc–amphibole, or olivine–amphibole, depending on the Fe:Mg ratio of the starting mix.

An effort was then made to synthesize olivine and orthopyroxene at 700°C from starting mixes containing ferrous oxalate, rather than metallic iron. In such starting mixes, CO_2 is evolved from ferrous oxalate, and thus the activity of H_2O in the fluid phase is reduced, resulting in an extension of the stability field of orthopyroxene to lower temperatures at the expense of hydrous phases.

IDENTIFICATION OF RUN PRODUCTS

All run products were examined by petrographic microscope and X-ray diffractometer (Fe $K\alpha$ radiation). The optical and X-ray properties of synthetic olivine and orthopyroxene are essentially the same as those for the natural minerals. Small differences in refractive indices and cell dimensions are due to the presence of minor elements in the natural minerals (Fisher and Medaris, 1969).

Compositions of olivine and orthopyroxene were determined by measurement of d_{130} in olivine and d_{610} in orthopyroxene, using SnO_2 ($d_{101} = 2.6428$) as an internal standard. These particular reflections were selected for determinative purposes because they are relatively intense and because there is no interference from other reflections in assemblages of olivine and orthopyroxene.

Six olivine and six orthopyroxene standards were synthesized in order to establish X-ray determinative curves. Measurements of d_{130} for

TABLE 1

Olivine and orthopyroxene standards
(900°C, P_{fluid} = 500 bars, FMQ buffer, FeKα radiation)

Run	Composition (Mole % Fo or En)	Duration (Hours)	
Olivine			d_{130}
51R	100	598	2.7645
77R2	80	556	2.7790
69R2	60	586	2.7907
73R2	40	621	2.8037
81R2	20	571	2.8153
FQI	0	168	2.8268
Orthopyroxene			d_{610}
113R2	90	497	2.8746
79R2	80	548	2.8774
114R2	70	497	2.8798
71R3	60	781	2.8837
83R2	50	528	2.8864
75R3	40	817	2.8900

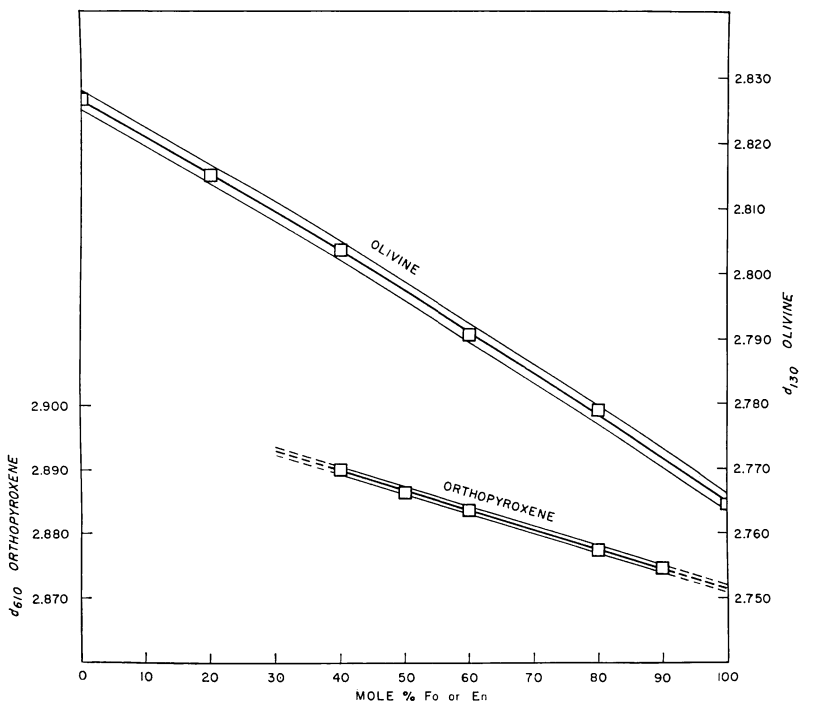

Fig. 1. X-ray determinative curves for synthetic olivine and orthopyroxene. Least squares regressions shown by heavy lines; 95 percent confidence intervals shown by light lines. Estimated error of each observation represented by size of symbol.

olivine and d_{610} for orthopyroxene are listed in table 1 and plotted in figure 1. Complete X-ray properties of synthetic olivine are reported elsewhere (Fisher and Medaris, 1969), and a description of X-ray and optical properties of synthetic orthopyroxene is in preparation.

The variation of d_{130} with olivine composition is a smooth curve (fig. 1), and analysis by the method of least squares gives

$$d_{130} = 2.8267 - 5.5 \times 10^{-4} X - 6.9 \times 10^{-7} X^2 \quad (1)$$

where X is mole percent forsterite. A 95 percent confidence interval for this equation corresponds to a precision of $\pm$ 2 mole percent forsterite in estimation of composition from measurements of d_{130}.

With the exception of En 70, which appears to be slightly off composition, measurements of d_{610} for orthopyroxene plot on a straight line (fig. 1). Neglecting En 70, least squares regression yields

$$d_{610} = 2.9020 - 3.06 \times 10^{-4} X \quad (2)$$

TABLE 2

Run data at 900°C, 500 bars fluid pressure, FMQ buffer

Run	Starting Material	Duration (hours)	Fluid	Run Products
125R	Fo90-En90 (mix)	326	H_2O	Fo 92.0 En 93.0
86R	Fo80-En80 (mix)	327	H_2O	Fo 81.0 En 83.5
87R	Fo60-En60 (mix)	327	H_2O	Fo 57.5 En 65.5
88R	Fo40-En40 (mix)	327	H_2O	Fo 36.0 En 44.5
E3	Fo 80 En 60	166	chloride solution	Fo 63.0 En 66.0
E6	Fo 40 En 60	166	chloride solution	Fo 45.0 En 56.0
E7R	Fo 40 En 20 (mix)	123	chloride solution	Fo 24.5 En 34.0
E8	Fo 20 En 40	166	chloride solution	Fo 25.0 En 34.5
E21R	Fo 60 En 80	335	H_2O	Fo 66.0 En 73.5
E22R	Fo 60 En 40	335	H_2O	Fo 51.0 En 53.0
E28	Fo 90 En 100	167	H_2O	Fo 94.0 En 95.0
E29R	Fo 40 En 20 (mix)	331	H_2O	Fo 28.5 En 34.0
E30R	Fo 100 En 80	331	H_2O	Fo 95.0 En 88.0
E34	Fo 100 En 90	69	chloride solution	Fo 97.0 En 92.5
E35	Fo 80 En 100	69	chloride solution	Fo 87.5 En 89.5
E38	Fo 90 En 100	165	H_2O	Fo 94.5 En 94.5
E39	Fo 80 En 100	70	chloride solution	Fo 89.0 En 92.0
E41R2	Fo 100 En 80	506	H_2O	Fo 95.5 En 91.0

where X is mole percent enstatite. The 95 percent confidence interval for this equation corresponds to a precision of ± 1.5 mole percent enstatite in estimation of composition from measurements of d_{610}.

EXPERIMENTAL RESULTS

Partitioning at 900°C.—Experimental data obtained at 900°C are listed in table 2 and illustrated in figure 2, in which the ratio of mole fraction of Fe and Mg in olivine, $(X_{Fe}/X_{Mg})_{OL}$, is plotted against the ratio of mole fraction of Fe and Mg in orthopyroxene, $(X_{Fe}/X_{Mg})_{OPX}$, on a logarithmic scale. This type of plot has been selected for use because points in the magnesium-rich portion of the diagram are spread apart, thereby facilitating comparison of experimental data with natural olivine–orthopyroxene assemblages, many of which are magnesium-rich.

The solid circles in figure 2 represent compositions of four olivine–orthopyroxene pairs synthesized from oxide starting mixes. Fitting a line by the method of least squares to the four synthesis points gives

$$\log\left(\frac{X_{Fe}}{X_{Mg}}\right)_{OL} = 0.1519 + 1.0836 \log\left(\frac{X_{Fe}}{X_{Mg}}\right)_{OPX} \qquad (3)$$

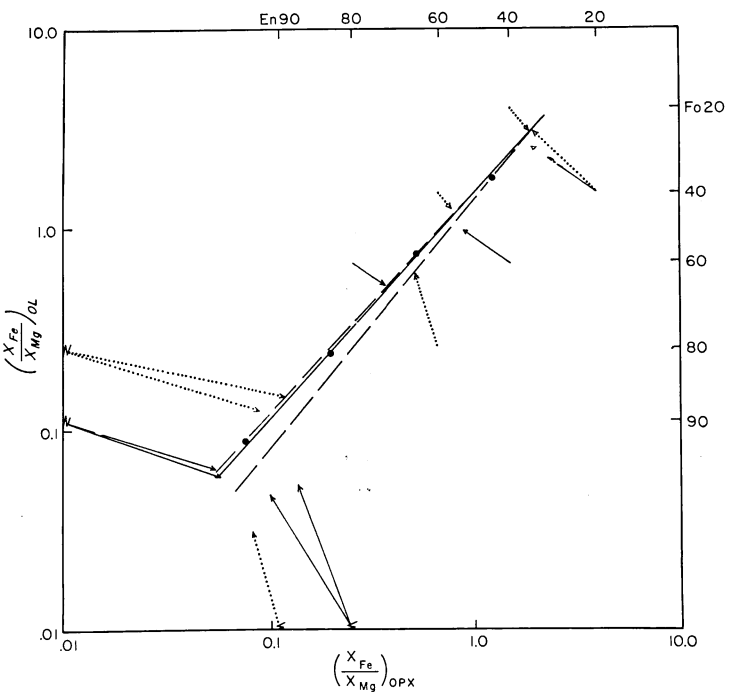

Fig. 2. Partitioning of Fe^{++} and Mg^{++} between synthetic olivine and orthopyroxene at 900°C, 500 bars fluid pressure, FMQ buffer. Solid Circles: synthesis assemblages; solid Arrows: reversal runs with H_2O; dotted Arrows: reversal runs with chloride solutions; light dashed lines: equilibrium limits defined by reversal runs; heavy solid line: partitioning expressed by equation (4) (see text).

However, because the mineral pairs under consideration are synthesis assemblages, it must be shown that equilibrium has been attained with respect to the Fe:Mg ratio of each phase.

Consequently, an attempt was made to demonstrate equilibrium by heating together synthetic olivine and orthopyroxene with different Fe:Mg ratios in the presence of either H_2O or 2M $(Mg,Fe)Cl_2$ solution. In run E3, for example, Fo 80, En 60, and chloride solution were maintained at 900°C for 166 hrs, resulting in a change of compositions to Fo 63 and En 66. By making reversal runs with starting materials of relatively Fe-rich olivine and Mg-rich orthopyroxene, and vice versa, equilibrium was approached from two directions, as indicated by the arrows in figure 2.

Equilibrium partitioning has not been completely established, because reversal runs with starting materials of Fo 100-En 90 and Fo 100-En 80 were more sluggish than the others. Nevertheless, the equilibrium position has been closely bracketed by reversal runs, and the partitioning curve must lie between the two dashed lines in figure 2.

TABLE 3

Run data at 800°C, 500 bars fluid pressure, FMQ buffer

Run	Starting Material	Duration (hours)	Fluid	Run Products
124R	Fo 90-En 90 (mix)	330	H_2O	Fo 91.5 En 90.0
90R	Fo 80-En 90 (mix)	353	H_2O	Fo 82.5 En 81.5
91R	Fo 60-En 60 (mix)	353	H_2O	Fo 56.0 En 66.0
92R	Fo 40-En 40 (mix)	353	H_2O	Fo 34.5 En 47.0
E12R	Fo 60 En 80	146	chloride solution	Fo 63.0 En 71.5
E13R	Fo 60 En 40	146	chloride solution	Fo 50.0 En 54.0
E16	Fo 20 En 40	50	chloride solution	Fo 25.5 En 33.0
E23R	Fo 80 En 100	187	chloride solution	Fo 80.0 En 87.0
E24R	Fo 80 En 60	186	chloride solution	Fo 77.0 En 66.5
E31	Fo 40 En 20 (mix)	96	chloride solution	Fo 28.0 En 36.0
E36	Fo 90 En 100	168	H_2O	Fo 94.0 En 97.5
E37	Fo 100 En 80	168	H_2O	Fo 98.0 En 87.0
E42R3	Fo 100 En 90	491	chloride solution	Fo 94.0 En 93.0
E43R2	Fo 40 En 20 (mix)	501	H_2O	Fo 27.5 En 36.5
E44R2	Fo 40 En 60	501	H_2O	Fo 43.0 En 59.5
E46	Fo 100 En 90	80	chloride solution	Fo 96.5 En 92.0
E47R	Fo 100 En 80	336	H_2O	Fo 97.5 En 86.5

Inasmuch as the synthesis assemblages plot within the limits defined by reversal runs, they are interpreted as being in equilibrium. Moreover, the final compositions of three reversal runs (E7R, E8, and E38) line up reasonably well with the four synthesis points, and least squares regression on these seven points yields

$$\log\left(\frac{X_{Fe}}{X_{Mg}}\right)_{OL} = 0.1630 + 1.1128 \log\left(\frac{X_{Fe}}{X_{Mg}}\right)_{OPX} \qquad (4)$$

When the errors involved in determination of olivine and orthopyroxene compositions are considered, the slight differences between equations (3) and (4) are insignificant.

It is suggested, therefore, that the equilibrium partitioning of Fe++ and Mg++ between olivine and orthopyroxene at 900°C is expressed by equation (4), which is shown by the solid line in figure 2. The coordinates at which the line terminates for iron-rich compositions, based on preliminary experiments, are only approximate. The partitioning line has not been extended into the most magnesium-rich portion of the diagram because of the lack of experimental control in that region.

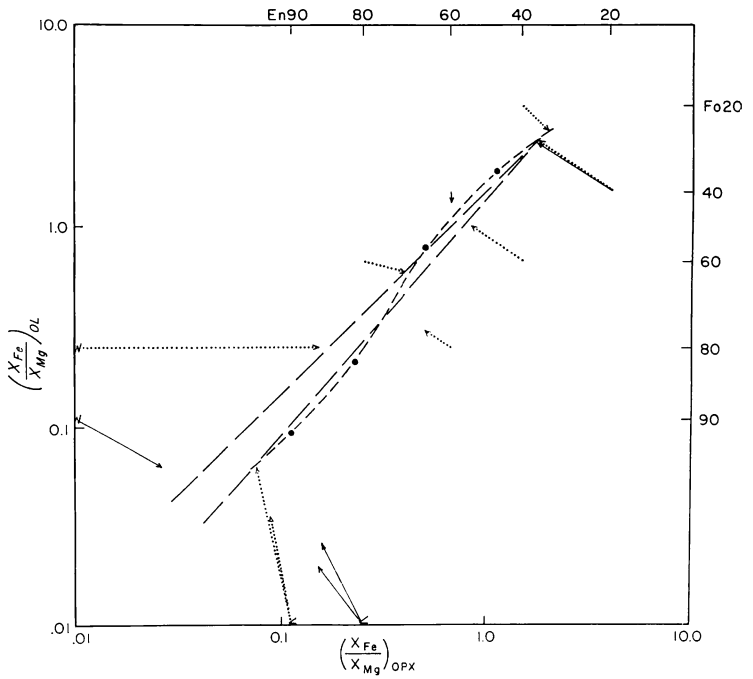

Fig. 3. Partitioning of Fe^{++} and Mg^{++} between synthetic olivine and orthopyroxene at 800°C, 500 bars fluid pressure, FMQ buffer. Solid Circles: synthesis assemblages; solid Arrows: reversal runs with H_2O; dotted Arrows: reversal runs with chloride solutions; light dashed lines: equilibrium limits defined by reversal runs; heavy dashed curve: hypothetical partitioning, assuming synthesis assemblages to be in equilibrium.

Partitioning at 800°C.—Experimental results for runs at 800°C are listed in table 3 and plotted in figure 3. Equilibration of reversal runs at 800°C was more sluggish than at 900°C, particularly in runs containing H_2O. Nevertheless, equilibrium partitioning has been reasonably well bracketed by reversal runs containing 2M chloride solutions, as shown by the light dashed lines in figure 3.

In contrast to the synthesis assemblages at 900°C, those at 800°C do not plot on a straight line in the partitioning diagram. One interpretation of the experimental data is that not all of the synthesis assemblages are in equilibrium, because three of the synthesis points fall outside the equilibrium limits defined by reversal runs. However, an alternative interpretation is that the synthesis assemblages are in equilibrium, plotting on a curve, shown by heavy dashes in figure 3, that is compatible with the reversal runs. On the basis of theoretical considerations given in the following section, the second interpretation does not appear to be valid, and it is concluded that the assemblages synthesized from oxide starting mixes at 800°C are not in equilibrium. However, despite this, the equilibrium partitioning at 800°C must lie between the two dashed lines in figure 3, as defined by reversal runs.

The line defined by equation (4), expressing partitioning at 900°C, plots within the equilibrium limits for partitioning at 800°C, and thus there is no discernible change in partitioning as a function of temperature over this 100° interval. However, considering the errors involved, a slight change in partitioning over this small temperature interval is not precluded.

Assemblages synthesized from oxalate starting mixes.—Coexisting olivine and orthopyroxene were synthesized from oxalate mixes and either H_2O or 2M $(Mg,Fe)Cl_2$ solutions at 900°, 800°, and 700°C. Interpretation of the experimental results is subject to two limitations. First, equilibrium for the synthesis assemblages has not been demonstrated by reversal runs. Second, due to difficulties in working with $Ag_{70}Pd_{30}$ tubing, runs were made in unbuffered Au capsules, and oxygen fugacity was not controlled.

Experimental data are presented in table 4 and plotted in figure 4. Run products at 800° and 900°C consisted of olivine and orthopyroxene, although cristobalite was present in the most iron-rich runs, and traces of an opaque mineral were found in a few runs. At 700°C orthopyroxene was synthesized only in the presence of chloride solutions, otherwise olivine-talc or olivine-amphibole appeared in the run products. In two of the magnesium-rich runs made with chloride solutions at 700°C monoclinic pyroxene, as well as rhombic pyroxene, was synthesized. In addition to silicates, a carbonate mineral was present in all run products at 700°C.

Examination of figure 4 does not reveal any consistent differences in the compositions of coexisting olivine and orthopyroxene synthesized from oxalate mixes at 900°, 800°, and 700°C. However, because oxygen fugacity was not controlled and equilibrium has not been demonstrated,

TABLE 4

Run data for oxalate mixes, $P_{fluid} = 500$ bars, no buffer

Run	Composition of oxalate starting mix	Duration (hrs)	Fluid	Run products
900°C				
OX2A	Fo 90-En 90	189	chloride solution	Fo 92.5 En 92.0
OX3	Fo 80-En 80	168	H_2O	Fo 82.0 En 80.0
OX4	Fo 80-En 80	168	chloride solution	Fo 82.0 En 80.5
OX10	Fo 60-En 60	167	chloride solution	Fo 65.0 En 66.5
OX13	Fo 60-En 60	167	H_2O	Fo 58.0 En 63.0
OX14	Fo 40-En 40	167	H_2O	Fo 37.0 En 43.5
OX25	Fo 40-En 40	168	chloride solution	Fo 38.0 En 47.0
800°C				
OX5	Fo 90-En 90	168	chloride solution	Fo 92.0 En 90.5
OX12	Fo 80-En 80	96	chloride solution	Fo 81.5 En 82.5
OX15	Fo 60-En 60	167	H_2O	Fo 60.0 En 61.0
OX16	Fo 40-En 40	167	H_2O	Fo 36.5 En 45.0
OX21	Fo 60-En 60	166	chloride solution	Fo 60.0 En 65.0
OX22A	Fo 40-En 40	163	chloride solution	Fo 37.5 En 43.5
OX22B	Fo 40-En 40	190	chloride solution	Fo 38.0 En 45.5
OX30	Fo 80-En 80	165	H_2O	Fo 82.0 En 79.5
OX31	Fo 80-En 80	165	chloride solution	Fo 82.5 En 82.5
OX34	Fo 20-En 20	162	chloride solution	Fo 19.0 En 28.0 Cristobalite
OX35	En 20	190	chloride solution	Fo 18.0 En 27.5 Cristobalite
OX36	En 30	163	H_2O	Fo 27.0 En 32.0
700°C				
OX8	Fo 90-En 90	157	chloride solution	Fo 91.5 En 94.0 Clinopyroxene Carbonate
OX9	Fo 80-En 80	157	chloride solution	Fo 83.0 En 84.5 Clinopyroxene Carbonate
OX23	Fo 60-En 60	166	chloride solution	Fo 62.0 En 64.5 Carbonate
OX24	Fo 40-En 40	166	chloride solution	Fo 37.0 En 47.5 Carbonate
OX33A	Fo 20-En 20	330	chloride solution	Fo 16.0 En 24.5 Carbonate

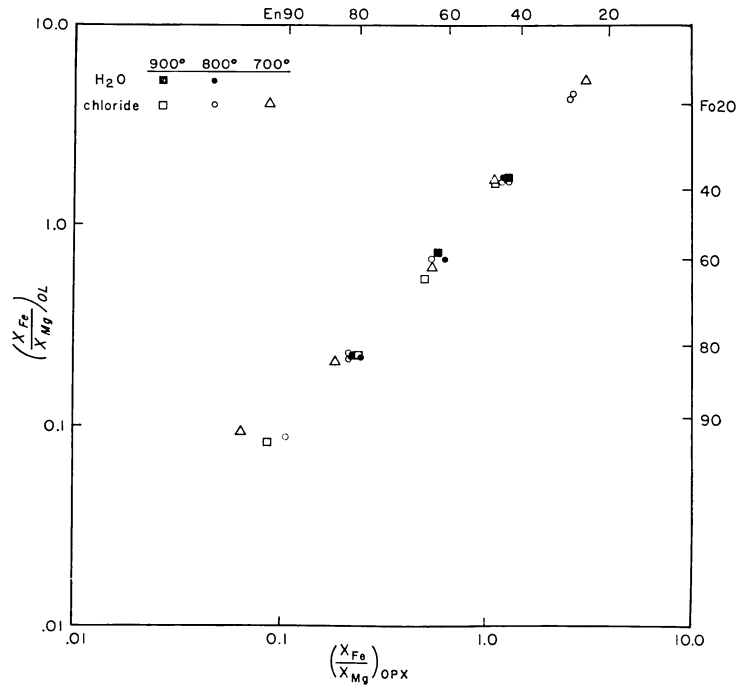

Fig. 4. Compositions of coexisting olivine and orthopyroxene synthesized from oxalate mixes at 500 bars fluid pressure, unbuffered.

it can only be concluded that partitioning of Fe^{++} and Mg^{++} between olivine and orthopyroxene does not change from 900° to 700°C in assemblages synthesized under these conditions.

THEORETICAL INTERPRETATION

The partitioning of Fe^{++} and Mg^{++} between olivine and orthopyroxene can be expressed by the reaction

$$\tfrac{1}{2}Mg_2SiO_4 + FeSiO_3 = \tfrac{1}{2}Fe_2SiO_4 + MgSiO_3 \qquad (6)$$

(Ramberg and DeVore, 1951; Mueller, 1964).

At equilibrium

$$\Delta G_{(6)}^{\circ} = -RT \ln \frac{a_{Fe}^{OL}\, a_{Mg}^{PX}}{a_{Mg}^{OL}\, a_{Fe}^{PX}} \qquad (7)$$

where $\Delta G_{(6)}^{\circ}$ is the change in standard free energy for reaction (6), R is the universal gas content, T is absolute temperature, and a_i^{α} is the activity of component i in phase α, with the standard state for the reaction defined in terms of the pure end members of the olivine and orthopyroxene solid solution series.

At a given temperature and pressure the activity quotient, K_a, is a constant,

$$\ln K_a = \ln \frac{a_{Fe}^{OL}\, a_{Mg}^{PX}}{a_{Mg}^{OL}\, a_{Fe}^{PX}} = -\frac{\Delta G_{(6)}^{\circ}}{RT} \qquad (8)$$

The variation of K_a with temperature is

$$\left(\frac{\partial \ln K_a}{\partial T}\right)_P = \frac{\Delta H^\circ}{RT^2} \tag{9}$$

where ΔH° is the change in standard enthalpy for reaction (6). Sufficient thermodynamic data for evaluation of equation (9) are not available, but the temperature effect on K_a can be interpreted from experimental data, discussed in the next section.

The influence of pressure on K_a is given by

$$\left(\frac{\partial \ln K_a}{\partial P}\right)_T = -\frac{\Delta V^\circ}{RT} \tag{10A}$$

where ΔV° is the change in molar volume for reaction (6). Based on the molar volumes of synthetic minerals,

$V^\circ_{Fo} = 43.62$ cc (Fisher and Medaris, 1969)
$V^\circ_{Fa} = 46.26$ cc (Fisher and Medaris, 1969)
$V^\circ_{En} = 31.39$ cc (Greenwood, 1963)
$V^\circ_{Fs} = 33.01$ cc (Burnham, 1965)

$\Delta V^\circ = -0.30$ cc for reaction (6) at 298°K, 1 atm. If ΔV° is assumed not to change with temperature and pressure, evaluation of equation (10A) from 1 atm to 10,000 atm at 800°K gives

$$K_{a\,(10{,}000\ atm)} = 1.05\ K_{a\,(1\ atm)} \tag{10B}$$

Ramberg and DeVore (1951, p. 200) and Mueller (1964, p. 195), using molar volume data for natural olivine and orthopyroxene, estimated from a similar calculation that

$$K_{a\,(10{,}000\ atm)} = 0.87\ K_{a\,(1\ atm)} \tag{10C}$$

The discrepancy between equations (10B) and (10C) is due to the differences in molar volumes of the synthetic and natural minerals. In any case, the effect of pressure on K_a is probably negligible at levels within the crust of the Earth.

Recently, Grover and Orville (1969) presented an elegant treatment of partitioning in terms of cation exchange between a single-site phase and a multi-site phase. The experimental results of the present study conform so well with the theoretical predictions made by Grover and Orville that their approach will be followed here. For a complete explanation of cation partitioning between single-site and multi-site phases, the reader is referred to their paper.

Olivine contains two cation sites, M_1 and M_2, each of which is symmetrically distinct (Bragg and Brown, 1926; Hanke, 1965). However, X-ray and Mossbauer studies have failed to reveal any partitioning of Fe^{++} and Mg^{++} between the two sites (Birle and others, 1968; Hanke, 1965; Bancroft, Maddock, and Burns, 1967), so Grover and Orville consider the two sites as energetically equivalent and treat olivine as a single-site phase.

On the other hand, the M_1 and M_2 sites in orthopyroxene are energetically, as well as structurally, distinct (Warren and Modell, 1930;

Ghose, 1965; Bancroft, Maddock, and Burns, 1967; Evans, Ghose, and Hafner, 1967), and orthopyroxene behaves as a double site phase.

Cation exchange between olivine and each site in orthopyroxene can be expressed by two reactions,

$$Mg^{OL} + (Fe^{M1})^{PX} = Fe^{OL} + (Mg^{M1})^{PX} \tag{11}$$

$$Mg^{OL} + (Fe^{M2})^{PX} = Fe^{OL} + (Mg^{M2})^{PX} \tag{12}$$

where $(Fe^{M1})^{PX}$ represents Fe^{++} in the M_1 site in orthopyroxene and Fe^{OL} represents Fe^{++} in olivine. The addition of equation (11) and (12) yields

$$2Mg^{OL} + (Fe^{M1} + Fe^{M2})^{PX} = 2Fe^{OL} + (Mg^{M1} + Mg^{M2})^{PX} \tag{13}$$

which represents the total cation exchange between olivine and orthopyroxene. Subtraction of equation (12) from equation (11) gives

$$(Fe^{M1} + Mg^{M2})^{PX} = (Mg^{M1} + Fe^{M2})^{PX} \tag{14}$$

which expresses the exchange of Fe^{++} and Mg^{++} between the M_1 and M_2 sites in orthopyroxene.

For olivine and orthopyroxene in equilibrium, the change in standard free energy for total cation exchange between the two phases is

$$\Delta G_T^\circ = \Delta G_{(11)} + \Delta G_{(12)}^\circ = \Delta G_{(13)}^\circ \tag{15}$$

or

$$\Delta G_T^\circ = -RT\left[\ln \frac{a_{Fe}^{OL}(a_{Mg}^{M1})^{PX}}{a_{Mg}^{OL}(a_{Fe}^{M1})^{PX}} + \ln \frac{a_{Fe}^{OL}(a_{Mg}^{M2})^{PX}}{a_{Mg}^{OL}(a_{Fe}^{M2})^{PX}}\right]. \tag{16}$$

If olivine and orthopyroxene are assumed to behave as ideal solid solutions (that is, the activity coefficients of Fe and Mg in olivine and orthopyroxene are all equal to 1.0), at $X_{Mg}^{PX} = 0.5$ equation (16) reduces to

$$\Delta G_T^\circ = -2RT \ln\left[\frac{1 - X_{Mg}^{OL}}{X_{Mg}^{OL}}\right] X_{Mg}^{PX} = 0.5 \tag{17}$$

where X_{Mg}^{OL} is the mole fraction of Mg in olivine, and X_{Mg}^{PX}, defined as $\frac{X_{Mg}^{M1} + X_{Mg}^{M2}}{2}$, is the average mole fraction of Mg in pyroxene.

The change in standard free energy for cation exchange between M_1 and M_2 in orthopyroxene is

$$\Delta G_E^\circ = 2RT \operatorname{acosh}$$

$$\left[\frac{\left(\frac{\partial X_{Mg}^{OL}}{\partial X_{Mg}^{PX}}\right)_{X_{Mg}^{PX} = 0.5}\left(1 - 2e^{-\frac{\Delta G_T^\circ}{RT}} + e^{-\frac{2\Delta G_T^\circ}{RT}}\right)}{\left(2e^{-\frac{3\Delta G_T^\circ}{2RT}} + 2e^{-\frac{\Delta G_T^\circ}{2RT}} - 4e^{-\frac{\Delta G_T^\circ}{RT}}\right)} - 1\right] \tag{18}$$

If the compositions of coexisting pairs of olivine and orthopyroxene, equilibrated at one temperature, are plotted on a graph with X_{Mg}^{OL} along the ordinate and X_{Mg}^{PX} along the abscissa, the values of X_{Mg}^{OL} and $(\partial X_{Mg}^{OL}/\partial X_{Mg}^{PX})$ at $X_{Mg}^{PX} = 0.5$ may be determined directly from the

graph. Using these values, ΔG_T° can be calculated from equation (17) and ΔG_E° from equation (18). Once ΔG_T° and ΔG_E° have been obtained, one can then compare the observed partitioning between olivine and orthopyroxene with the theoretical partitioning, given by Grover and Orville as

$$X_{Mg}^{PX} = \tfrac{1}{2}\left[\frac{X_{Mg}^{OL}\exp(\Delta G_E^\circ - \Delta G_T^\circ)/2RT}{X_{Mg}^{OL}\exp(\Delta G_E^\circ - \Delta G_T^\circ)/2RT + (1 - X_{Mg}^{OL})} + \frac{X_{Mg}^{OL}\exp(-\Delta G_T^\circ - \Delta G_E^\circ)/2RT}{X_{Mg}^{OL}\exp(-\Delta G_T^\circ - \Delta G_E^\circ)/2RT + (1 - X_{Mg}^{OL})}\right] \quad (19)$$

based on the ideal single-site–double-site model.

A comparison between the experimental data obtained at 900°C and partitioning predicted on the basis of the ideal single-site–double-site model is shown in figure 5. From equation (4) $X_{Mg}^{OL} = 0.4073$ when $X_{Mg}^{PX} = 0.5000$. Differentiating X_{Mg}^{OL} with respect to X_{Mg}^{PX} in equation (4), $(\partial X_{Mg}^{OL}/\partial X_{Mg}^{PX})_{X_{Mg}^{PX}=0.5} = 1.0652$. By substituting these values in equations (17) and (18), one obtains $\Delta G_{T(900)}^\circ = -1750$ cal/gfw and

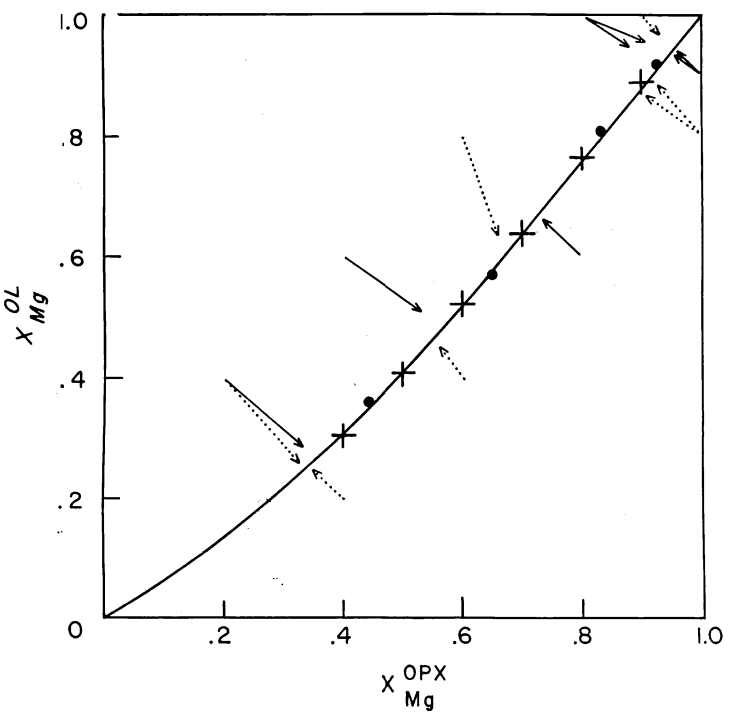

Fig. 5. Comparison of experimental and theoretical partitioning. Theoretical partitioning at 900°C is shown by the solid curve. Experimental partitioning expressed by equation (4) is represented by crosses at intervals of 0.1 X_{Mg}^{OPX}. Solid circles, synthesis assemblages; solid arrows, reversal runs with H_2O; dashed arrows, reversal runs with chloride solutions.

$\Delta G_{E(900)}^{\circ} = -2940$ cal/gfw for cation exchange between synthetic olivine and orthopyroxene. Equation (19) can now be used to derive the theoretical partitioning curve, shown in figure 5 as a solid line. Equation (4), represented by crosses at intervals of 0.1 X_{Mg}^{PX}, is in close agreement with the theoretical partitioning curve in the compositional range for which there is experimental control, that is, for $0.32 < X_{Mg}^{OPX} < 0.96$. Thus the partitioning of Fe^{++} and Mg^{++} between olivine and orthopyroxene appears to be explained adequately in terms of cation exchange between a single-site and a double-site phase, as postulated by Grover and Orville.

The experimental data obtained at 800°C has also been compared with the theoretical model. The synthesis assemblages were assumed to be in equilibrium, and the heavy dashed curve in figure 3 was replotted on a diagram similar to figure 5. Substitution of values for X_{Mg}^{OL} and $(\partial X_{Mg}^{OL}/\partial X_{Mg}^{PX})$ at $X_{Mg}^{PX} = 0.5$ in equations (17) and (18) gave $\Delta G_{E(800)}^{\circ} = 2RT\text{acosh}(0.9357)$. This expression cannot be correct, because acosh must be $\geqslant 1.0$. It is therefore concluded that equilibrium was not attained in olivine–orthopyroxene assemblages synthesized at 800°C.

Throughout this discussion it has been assumed that olivine and orthopyroxene constitute ideal solid solution series. From high-temperature experimental studies in the system MgO–"FeO"–SiO_2 Nafziger and Muan (1967) concluded that pyroxene solid solution is practically ideal, but that olivine solid solution shows a moderate positive deviation from ideality. Fisher and Medaris (1969) also suggest that olivine is slightly non-ideal on the basis of unit cell volume determinations. In view of the possibility that olivine might not be ideal, the close agreement between the experimental and theoretical partitioning curves in figure 5 is surprising, considering that the theoretical curve was calculated on the assumption that both silicates are ideal. The close correspondence between the two curves indicates that if olivine is indeed non-ideal, it must be only slightly so.

There is good agreement between ΔG_T° determined at 900°C in this study and ΔG_T° given by Larimer (1968) at higher temperatures, as seen from table 5. For purposes of comparison, values of ΔG_T° reported

TABLE 5

Comparison of experimental determinations of ΔG_T°

	ΔG_T° (cal/gfw)	
T°C	This study	Larimer
900	−1750	−1260*
1100		−1460 ± 200
1200		−1540 ± 200
1300		−1660 ± 200

* By extrapolation from values at 1100°, 1200°, and 1300°.

TABLE 6

Experimental data, other investigations

T°C	P_{total}	Log fo_2	Olivine (mole % Fo)	Pyroxene (mole % En)
Muan and Osborn (cited by Speidel and Osborn, 1967)				
1375	1 atm	−0.7 atm	91.5	93.5
1285		−5.6	59.5	69.5
1255		−7.1	53.0	56.0
Speidel and Osborn (1967)				
1350	1 atm	−0.7 atm	91	93.5
1126		−0.7	90	94
1240		−6.3	64	69
1240		−6.3	64	68
1240		−7.3	54	57
Nafziger and Muan (1967)				
1200	1 atm	in	95	95
1200		equilibrium	89	89
1200		with	85	86
1200		metallic	74	78
1200		iron	70	76
1200			64	71
1200			57	60
1200			55	60
1200			51	55
1200			44	48
1200			38	44
Larimer (in press)				
1100	1 atm	−16.45 atm	97.9	98.1
		−15.59	94.3	94.8
		−15.33	92.1	92.9
		−15.33	92.4	93.2
		−15.01	88.7	90.0
		−14.84	86.4	88.0
		−14.58	80.5	82.9
1200	1 atm	−15.15 atm	98.2	98.3
		−14.29	95.0	95.5
		−14.03	94.0	94.4
		−13.91	91.7	92.7
		−13.54	83.7	85.6
		−13.00	65.2	69.4
1300	1 atm	−14.01 atm	97.2	97.5
		−14.01	97.4	97.6
		−13.16	92.7	93.5
		−13.16	92.5	93.4
		−12.90	91.9	92.7
		−12.57	83.3	85.3
Ernst (1960)				
940	1000 bars	−6.35 bars	95 ± 5	98 ± 2
912		−12.9	73 ± 10	79 ± 3
900		−14.87	65 ± 10	73 ± 3
Green and Ringwood (1967)				
1290	9000 bars	unspecified	87.2	87.3
1270			86.4	86.4
1250			85.3	84.9

by Larimer have been doubled, because equation (13) expresses the total cation exchange between olivine and orthopyroxene in terms of two atoms each of Fe and Mg, whereas Larimer considers the exchange reaction in terms of only 1 atom.

COMPARISON WITH OTHER EXPERIMENTAL STUDIES

Data on Fe^{++}–Mg^{++} partitioning between olivine and orthopyroxene at liquidus temperatures and 1 atm pressure have been reported Muan (1967), and Larimer (1968). Additional data at $P_{fluid} = 1000$ Muan (1967), and Larimer (in press). Additional data at $P_{fluid} = 1000$ bars and $P_{total} = 9000$ bars have been given by Ernst (1960) and Green and Ringwood (1966), respectively. By comparison of the information available in these studies with the data at 900°C, it is now possible to evaluate the temperature dependence of partitioning and thereby to test the effectiveness of an olivine–orthopyroxene geothermometer.

Experimental data from other investigations are summarized in table 6 and compared with the 900°C data in figures 6A, 6B, and 6C. In each figure the 900°C partitioning curve shown is that expressed by equation (4). At coordinates less than (0.05, 0.05) there is no experimental control on the position of the 900°C partitioning curve. However, because the experimental data are in excellent agreement with partitioning predicted theoretically by equation (19), the experimental partitioning curve has been extended to coordinates less than (0.05, 0.05) according to theoretical estimates.

There is a remarkable similarity between partitioning at 900° and that at 1100°, 1200°, and 1300°C, established by Larimer (1968) (fig. 6A). Close agreement is also found between partitioning at 900° and that at 1200°C, given by Nafziger and Muan (1967) (fig. 6B). Apparently, no significant change in partitioning occurs over these relatively large temperature intervals. The remaining experimental data are shown in figure 6C for comparison.

At liquidus temperatures olivine has a slightly greater Fe:Mg ratio than does associated orthopyroxene. If partitioning were sensitive to changes in temperature, one would expect that the difference between Fe:Mg ratios in coexisting olivine and orthopyroxene would become more pronounced with a decrease in temperature, resulting in an upward shift in position of the partitioning curve in a log–log plot. It was pointed out previously that the partitioning curve at 900°, expressed by equation (4), coincides closely with the upper equilibrium limit defined by reversal runs. Thus, even though equilibrium has not been completely established at 900°, the partitioning curve for this temperature represents a limit to any possible upward shift of partitioning curves accompanying a decrease in temperature from 1300° to 900°C.

It is concluded that partitioning of Fe^{++} and Mg^{++} between olivine and orthopyroxene does not change appreciably as a function of temperature in the interval from 900° to 1300°C and thus can not be used in geothermometry.

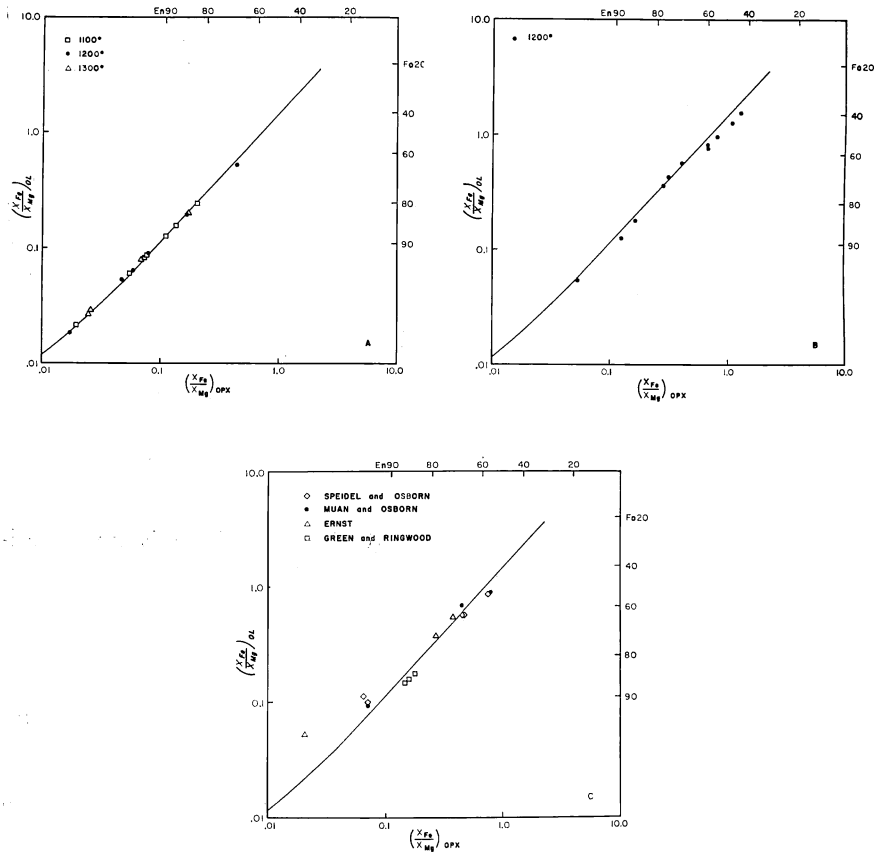

Fig. 6. Comparison of experimental partitioning at 900°C with results from other experimental investigations. Solid line is partitioning at 900°C. A. data from Larimer (1968); B. data from Nafziger and Muan (1967); C. data from Speidel and Osborn (1967), Muan and Osborn (1956), Ernst (1960), and Green and Ringwood (1967). See table 6 for experimental conditions.

Up to this point the temperature dependence of partitioning has been examined by comparison of experimental data expressed in terms of mole fractions of Fe and Mg. If the olivine solid solution series is truly non-ideal, as suggested by Nafziger and Muan (1967), the temperature dependence of partitioning should be evaluated in terms of the activities of Fe and Mg in olivine, rather than mole fractions. The activity coefficients for Fe and Mg in olivine at 900° are unknown, but Larimer (1968), utilizing activity coefficients determined by Nafziger and Muan at 1150° and 1200°C, calculated the activity quotient, K_a, for coexisting olivine and pyroxene equilibrated at 1100°, 1200°, and 1300°C, and found K_a to be the same, within experimental error, at each of the three temperatures.

Consequently, partitioning of Fe^{++} and Mg^{++} between olivine and orthopyroxene does not appear to be significantly temperature dependent, whether expressed in terms of mole fractions in the temperature interval, 900° to 1300°C, or given in terms of activities in the interval, 1100° to 1300°C.

A problem is encountered in attempting direct comparison of partitioning at 900°C with that at liquidus temperatures, because rhombic pyroxene is the stable pyroxene polymorph at 900°C, whereas clinopyroxene, the result of inversion from protoenstatite, is generally the quench product in runs made at liquidus temperatures (Boyd and Schairer, 1964, p. 297). Larimer (1968) found rhombic pyroxene and Ca-free clinopyroxene, both apparently in equilibrium with olivine, in two iron-rich runs at 1100°C. Microprobe analyses indicated that compositions of the coexisting pyroxenes were the same within experimental error, $\pm$ 5 percent of iron content of the pyroxenes. In addition, rhombic pyroxene alone was present with olivine in the most iron-rich run at both 1100° and 1200°C. Partitioning between olivine and rhombic pyroxene in these two runs is essentially identical with partitioning between olivine and clinopyroxene in the other runs at 1100° and 1200°C (see fig. 6A).

It appears, then, that partitioning of Fe^{++} and Mg^{++} between olivine and pyroxene is not significantly affected by the type of pyroxene polymorph in the assemblage, and comparison of partitioning between olivine and pyroxene at 900°C with that at liquidus temperatures seems to be valid.

Another factor that must be considered in the comparison of partitioning data is the possible influence of oxygen fugacity on the compositions of coexisting olivine and orthopyroxene. Iron occurs mainly as Fe^{++} in natural olivine and orthopyroxene, although orthopyroxene may contain small amounts of Fe^{+++} (Deer, Howie, and Zussman, 1962, v. 1, p. 5-6; v. 2, p. 15-22). However, in synthetic olivine and orthopyroxene, containing only the cations Si, Mg, and Fe, virtually all the iron must be divalent in order to maintain a balance of ionic charges. Consequently, Fe^{++}–Mg^{++} partitioning between olivine and orthopyroxene should not be affected appreciably by variations in oxygen fugacity, provided the oxygen fugacity remains at levels at which the silicates are stable.

The available experimental data tend to confirm this idea, since partitioning for olivine and pyroxene in equilibrium with magnetite, determined by Speidel and Osborn (1967) and Muan and Osborn (1956), is essentially the same as that shown by Nafziger and Muan (1967) and Larimer (1968) for the silicates in equilibrium with metallic iron (compare figs. 6A, 6B, and 6C).

GEOLOGIC APPLICATION

Temperatures of equilibration for rocks containing olivine and orthopyroxene cannot be determined on the basis of the compositions of

these two minerals. However, as illustrated in figure 7, comparison of the compositions of natural olivine–orthopyroxene pairs with the experimental partitioning curve may indicate whether or not the natural pairs crystallized under equilibrium conditions.

Compositions of olivine and orthopyroxene from 114 chondritic meteorites, taken from electron microprobe investigations by Keil and Fredriksson (1964) and Van Schmus and Koffman (1967; and personal

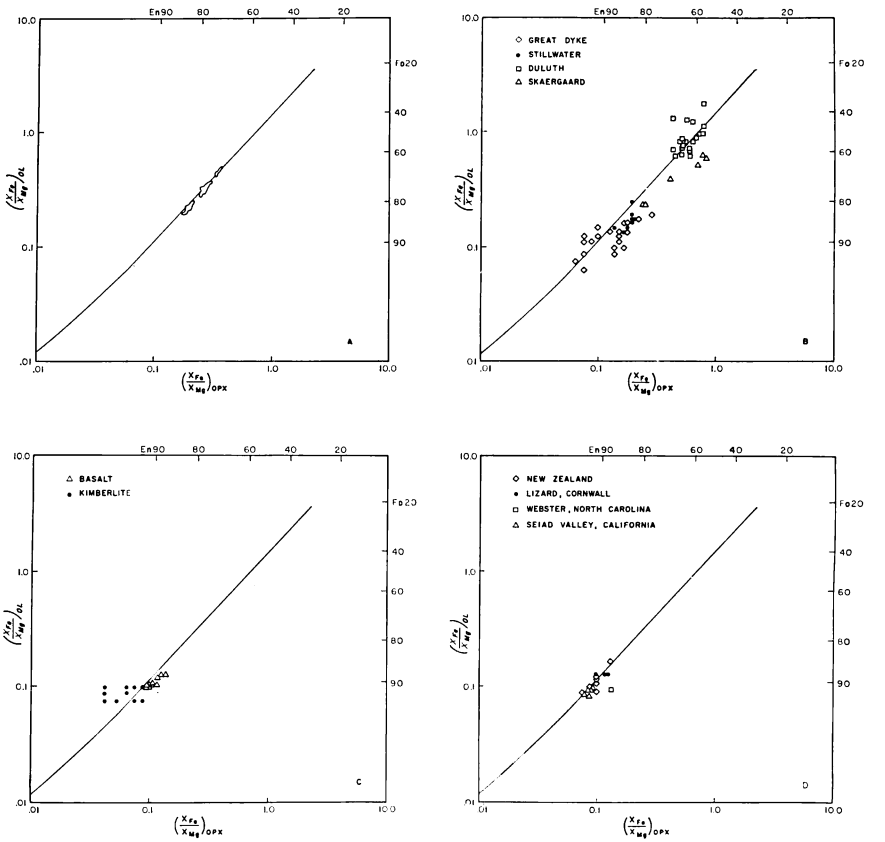

Fig. 7. Comparison of experimental partitioning at 900°C with compositions of coexisting olivine and orthopyroxene in natural rocks. Experimental curve is shown by solid line.

A. Chondritic meteorites (Keil and Fredriksson, 1964; Van Schmus and Koffman, personal commun.). Compositions of 114 olivine–orthopyroxene pairs plot within the enclosed areas.

B. Stratiform basic intrusions (Brown, 1957; Hess, 1951, 1960; Snyder, 1959; Taylor, 1964; Wager and Deer, 1939; Worst, 1958).

C. Peridotite inclusions in basalt and kimberlite (O'Hara, 1963; Ross, Foster, and Myers, 1954; Wilshire and Binns, 1961).

D. Alpine peridotites (Bartholome, 1962; Challis, 1965; Green, 1964; Medaris, unpublished).

communication), are plotted in figure 7A. The 86 specimens examined by Keil and Fredriksson show a wide range in degree of metamorphism as indicated by their textural variations. The remaining 28 specimens, described by Van Schmus and Koffman are strongly recrystallized (type-6) chondrites. Although Keil and Fredriksson have described a number of chondrites in which olivine and orthopyroxene compositions are variable, only specimens containing homogeneous olivine and orthopyroxene are shown in figure 7A. The close agreement between the plot for olivine–orthopyroxene pairs in chondrites and the experimental partitioning curve suggests that the silicate phases are in equilibrium. In addition, it seems unlikely that all chondrites have been subjected to the same temperature of equilibration, and therefore the fact that all the points plot close to the experimental curve supports the proposition that Fe++–Mg partitioning between olivine and orthopyroxene is not appreciably temperature-dependent.

Compositions of olivine and orthopyroxene from the Duluth gabbro (Snyder, 1959; Taylor, 1964), the Great Dyke of Southern Rhodesia (Hess, 1951; Worst, 1958), the Skaergaard intrusion (Wager and Deer, 1939; Brown, 1957), and the Stillwater complex (Hess, 1960) are shown in figure 7B. Some compositional data are based on chemical analyses; others, on optical determinations. Scatter of points about the experimental partitioning curve indicates that many of the olivine–orthopyroxene pairs are not in equilibrium, although some scatter may be due to errors in compositional determinations. For the majority of the disequilibrium pairs, orthopyroxene is enriched in iron with respect to olivine, and the corresponding points fall below the experimental curve. Textural features, such as embayment of olivine by pyroxene, have been interpreted by Hess (1960, p. 59) and Jackson (1961, p. 47) as evidence for reaction relation between olivine and silicate melt in stratiform basic intrusives. If reaction could not go to completion because of crystal settling or compositional zoning of olivine, iron-enrichment of the later pyroxene would result.

Based on chemical analyses by Ross, Foster, and Myers (1954) and optical determinations by Wilshire and Binns (1961), olivine–orthopyroxene pairs from peridotite nodules in basalt plot close to, but slightly below, the experimental partitioning curve (fig. 7C). In contrast, the compositions of olivine and orthopyroxene from peridotite nodules in kimberlite, based on optical data by O'Hara (1963), tend to plot above the experimental curve (fig. 7C). Although the pressure-dependence of partitioning is slight, as previously explained, the possible effect of high pressures on compositions of coexisting silicates in peridotite nodules from basalt and kimberlite should not be overlooked. The departure of olivine–orthopyroxene pairs from the experimental partitioning curve in figure 7C may be due to shifts in partitioning in response to pressure, rather than to disequilibrium. If this interpretation is correct, the pressure environment from which peridotite nodules in basalt is derived

favors a downward shift in the partitioning curve, but at the higher pressures presumed for peridotite nodules in kimberlite, an upward shift in the partitioning curve is favored. The opposite effects of pressure on partitioning in the two cases can possibly be explained by the minor element content of olivine and orthopyroxene and the influence of these elements on partial molar volumes. For example, Ringwood, MacGregor, and Boyd (1964) have demonstrated that the following mineral assemblages are stable in a rock of pyrolite composition with increasing temperature and pressure along a typical oceanic geothermal gradient: olivine + two pyroxenes + spinel, olivine + aluminous pyroxenes, olivine + two pyroxenes (less than 1 percent Al_2O_3) + pyrope-rich garnet. The change in volume for exchange of Fe++ and Mg++ olivine and orthopyroxene containing minor elements is given by

$$\Delta\overline{V} = \tfrac{1}{2}\,\overline{V}_{Fa}{}^{OL} + \overline{V}_{En}{}^{OPX} - \tfrac{1}{2}\,\overline{V}_{Fo}{}^{OL} - \overline{V}_{Fs}{}^{OPX} \qquad (20)$$

where $\overline{V}_A{}^{\alpha}$ is the partial molar volume of component A in phase α. The influence of pressure on partitioning is then expressed by

$$\left(\frac{\partial \ln K_a}{\partial P}\right)_T = -\frac{\Delta\overline{V}}{RT} \qquad (21)$$

If the partial molar volumes of the pyroxene end members, $MgSiO_3$ and $FeSiO_3$, do not change by exactly the same amount with substitution of aluminum, then $\Delta\overline{V}$ and $(\partial \ln K_a/\partial P)_T$ will be different for each of the three pyrolite mineral assemblages.

With the exception of one point, olivine–orthopyroxene pairs from alpine peridotites (Bartholomé, 1962; Green, 1964; Challis, 1965; and Medaris, unpublished) cluster about the experimental curve (fig. 7D) and presumably represent equilibrium assemblages.

References

Bancroft, G. M., Maddock, A. G., and Burns, R. G., 1967, Applications of the Mössbauer effect to silicate mineralogy I. Iron silicates of known crystal structure: Geochim. et Cosmochim. Acta, v. 31, p. 2219-2246.

Bartholomé, Paul, 1962, Iron-magnesium ratio in associated pyroxenes and olivines, in Engel, A. E. J., and Engel, C. G., Petrologic studies—a volume in honor of A. F. Buddington: New York, Geol. Soc. America, p. 1-20.

Birle, J. D., Gibbs, G. V., Moore, P. B., and Smith, J. V., 1968, Crystal structures of natural olivines: Am. Mineralogist, v. 53, p. 807-824.

Bowen, N L., and Schairer, J. F., 1935, The system, MgO–FeO–SiO_2: Am. Jour. Sci., v. 229, p. 151-217.

Boyd, F. R., and Schairer, J. F., 1964, The system $MgSiO_3$–$CaMgSi_2O_6$: Jour. Petrology, v. 5, p. 275-309.

Bragg, W. L., and Brown, G. B., 1926, Die Struktur des Olivins: Zeitschr. Kristallographie, v. 63, p. 538-556.

Brown, G. M., 1957, Pyroxenes from the early and middle stages of fractionation of the Skaergaard intrusion, east Greenland: Mineralog. Mag., v. 31, p. 511-543.

Burnham, C. W., 1965, Ferrosilite: Carnegie Inst. Washington Year Book 64, p. 202-204.

Challis, G. A., 1965, The origin of New Zealand ultramafic intrusions: Jour. Petrology, v. 6, p. 322-364.

Craig, Harmon, 1964, Petrological and compositional relationships in meteorites, *in* Craig, Harmon, Miller, S. L., and Wasserburg, G. J., eds., Isotopic and cosmic chemistry: Amsterdam, North Holland Pub. Co., p. 401-451.

Deer, W. A., Howie, R. A., and Zussman, J., 1963, Rock-forming minerals, 5 v.: New York, John Wiley and Sons, Inc.

Ernst, W. G., 1960, The stability relations of magnesioriebeckite: Geochim. et Cosmochim. Acta, v. 19, p. 10-40.

Eugster, H. P., 1957, Heterogeneous reactions involving oxidation and reduction at high pressures and temperatures: Jour. Chem. Physics, v. 26, p. 1760-1761.

———— 1959, Reduction and oxidation in metamorphism, *in* Abelson, P. H., ed., Researches in Geochemistry: New York, John Wiley and Sons, Inc., p. 397-426.

Eugster, H. P., and Wones, D. R., 1962, Stability relations of the ferriginous biotite, annite; Jour. Petrology, v. 3, p. 82-125.

Evans, B. J., Ghose, S., and Hafner, S., 1967, Hyperfine splitting of Fe^{57} and Mg–Fe order-disorder in orthopyroxenes (Mg SiO_3–$FeSiO_3$ solid solution): Jour. Geology, v. 75, p. 306-322.

Fisher, G. W., and Medaris, L. G., Jr., 1969, Cell dimensions and X-ray determinative curve for synthetic Mg–Fe olivines: Am. Mineralogist, v. 54, p. 741-753.

Ghose, S., 1965, Mg^{2+}–Fe^{2+} order in an orthopyroxene $Mg_{0.93}$ $Fe_{1.07}Si_2O_6$: Zeitschr. Kristallographie, v. 122, p. 81-99.

Green, D. H., 1964, The petrogenesis of the high-temperature peridotite intrusion in the Lizard area, Cornwall: Jour. Petrology, v. 5, p. 134-188.

Green, D. H., and Ringwood, A. E., 1967, The genesis of basaltic magmas: Contr. Mineralogy Petrology, v. 15, p. 103-190.

Greenwood, H. J., 1963, The synthesis and stability of anthophyllite: Jour. Petrology, v. 4, p. 317-351.

Grover, J. E., and Orville, P. M., 1969, The partitioning of cations between coexisting single- and multi-site phases with application to the assemblages: orthopyroxene–clinopyroxene and orthopyroxene–divine: Geochim. et Cosmochim. Acta, v. 33, p. 205-226.

Hanke, K., 1965, Beiträge zu Kristallstrukturen vom Olivin-Typ: Beitr. Mineralogie Petrographie, v. 11, p. 535-558.

Hess, H. H., 1951, Vertical mineral variation in the Great Dyke of Southern Rhodesia: Geol. Soc. South Africa Trans. and Proc., v. 53, p. 159-167.

———— 1960, Stillwater igneous complex, Montana: Geol. Soc. America Mem. 80, 230 p.

Jackson, E. D., 1961, Primary textures and mineral associations in the ultramafic zone of the Stillwater complex, Montana: U. S. Geol. Survey Prof. Paper 358, 106 p.

Keil, Klaus, and Fredriksson, K., 1964, The iron, magnesium and calcium distribution in coexisting olivines and rhombic pyroxenes of chondrites: Jour. Geophys. Research, v. 69, p. 3487-3515.

Larimer, J. W., 1968, Experimental studies on the system Fe–MgO–SiO_2–O_2 and their bearing on the petrology of chondritic meteorites: Geochim. et Cosmochim. Acta, v. 32, p. 1187-1207.

Muan, Arnulf, and Osborn, E. F., 1956, Phase equilibria of liquidus temperatures in the system MgO–FeO–Fe_2O_3–SiO_2: Am. Ceramic Soc. Jour. v. 39, p. 121-137.

Mueller, R. F., 1964, Phase equilibria and the crystallization of chondritic meteorites: Geochim. et Cosmochim. Acta, v. 28, p. 189-207.

Nafziger, R. H., and Muan, Arnulf, 1967, Equilibrium phase compositions and thermodynamic properties of olivines and pyroxenes in the system MgO–"FeO"–SiO_2: Am. Mineralogist, v. 52, p. 1364-1385.

O'Hara, M. J., 1963, Distribution of iron between coexisting olivines and calcium-poor pyroxenes in peridotites, gabbros, and other magnesium environments: Am. Jour. Sci., v. 261, p. 32-46.

Orville, P. M., 1963, Alkali ion exchange between vapor and feldspar phases: Am. Jour. Sci., v. 261, p. 201-237.

Ramberg, H., and DeVore, 1951, The distribution of Fe^{++} and Mg^{++} in coexisting olivines and orthopyroxenes: Jour. Geology, v. 59, p. 193-210.

Ringwood, A. E., 1961, Chemical and genetic relationships among meteorites: Geochim. et Cosmochim. Acta, v. 24, p. 159-197.

Ringwood, A. E., MacGregor, I. D., and Boyd, R. F., 1964, Petrological constitution of the upper mantle: Carnegie Inst. Washington Year Book 63, p. 147-152.

Ross, C. S., Foster, M. D., and Myers, A. T., 1954, Origin of dunites and of olivine-rich inclusions in basaltic rocks: Am. Mineralogist, v. 39, p. 693-737.

Snyder, J. L., 1959, Distribution of certain elements in the Duluth complex: Geochim. et Cosmochim. Acta, v. 16, p. 243-277.

Speidel, D. H., and Osborn, E. F., 1967, Element distribution among co-existing phases in the system MgO–FeO–Fe_2O_3–SiO_2 as a function of temperature and oxygen fugacity: Am. Mineralogist, v. 52, p. 1139-1152.

Taylor, R. B., 1964, Geology of the Duluth gabbro complex: Minnesota Geol. Survey Bull. 44, 63 p.

Van Schmus, W. R., and Koffman, D., 1967, Fe^{++} and Mg^{++} equilibration temperatures in chondritic meteorites: Science, v. 155, p. 1009-1101.

Wager, L. R., and Deer, W. A., 1939, The petrology of the Skaergaard intrusion, Kangerdlugsuag, east Greenland: Medd. om Grönland, v. 105, 335 p.

Warren, B. E., and Modell, D. I., 1930, The structure of enstatite $MgSiO_3$: Zeitschr. Kristallographie, v. 75, p. 1-14.

Wilshire, H. G., and Binns, R. A., 1961, Basic and ultrabasic xenoliths from volcanic rocks of New South Wales: Jour. Petrology, v. 2, p. 185-208.

Wones, D. R., and Gilbert, M. C., 1967, The stability of fayalite: Carnegie Inst. Washington Year Book 66, p. 402-403.

Worst, B. G., 1958, The differentiation and structure of the Great Dyke of Southern Rhodesia: Geol. Soc. South Africa Trans. and Proc., v. 61, p. 274-358.